Directional Filtering in Edge Detection

Andrew P. Papliński

***Abstract*— Two-dimensional (2-D) edge detection can be performed by applying a suitably selected optimal edge half-filter in n directions. Computationally, such a two-dimensional n-directional filter can be represented by a pair of real masks, that is, by one complex-number matrix, regardless of the number of filtering directions, n. Specific calculations of the edge strength were conducted using a 2-D tridirectional filter based on a Petrou–Kittler one-dimensional (1-D) detector optimized for the ramp edges, which are characteristic of posterior eye capsule images that were used here as a test set. In applications to image segmentation, tridirectional filtering results in co-occurrence arrays of low dimensionality.**

***Index Terms*— Conjugate images, directional filtering, edge detection, posterior capsule images.**

I. Introduction

This correspondence is focused on the use of directional filters for edge detection. The method considered in this work stems from our work on the segmentation of a class of medical images, namely, posterior eye capsule images taken after a cataract operation [1], [2].

If we ignore the noise present in images, edge detection can be based primarily on the computation of the gradient of intensity with subsequent thresholding of its magnitude. For this purpose the popular filters, like the Sobel filter [4], are used. Hence, a typical simple method of obtaining an edge strength map is based on the estimation of two components of the intensity gradient vector using horizontal and vertical Sobel masks.

Taking noise and edge imperfection into consideration, edge filters are traditionally constructed so as to improve the suppression of unwanted disturbances by appropriate lowpass filtering. The idea has originated perhaps from the concept of stochastic gradient [5] and from work of Marr and Hildreth [6], and in its current form was introduced by Canny [7] and developed further in many works using various criteria of optimality of the edge detection process. Following a classification of the optimal one-dimensional (1-D) edge filters presented by Heijden [8], the following operators are considered to be the main contenders: Canny [7] and its version by Deriche [9], Shen–Castan [10], [11], (see also [12]), Sarkar–Boyer [13], Boie–Cox [14], Spacek [15], Petrou-Kittler [16], and the CVM detector of Heijden [8]. The above filters were primarily constructed as 1-D filters and then extended appropriately into two dimensions. Typically, a two-dimensional (2-D) edge filter is formed by the following two-step procedure. First, a 1-D optimal filter is expanded in the direction perpendicular to the edge, and a windowed projection function is applied in the direction parallel to the edge. This results in a 2-D filtering component. In the second step, two such 2-D filtering components are applied in orthogonal directions to estimate the magnitude (and direction) of 2-D edges. A relevant example can be found in [13].

These two basic aspects, namely, utilization of an optimal 2-D edge filtering component, and its application in two orthogonal directions, are also present in our approach with two notable modifications. Firstly, the 2-D filtering component utilizes only the positive half of the optimal 1-D edge filter, and secondly, the 2-D component is applied in a selected number of directions, which, starting with three, results in the tridirectional filtering. We may say that in our approach we combine the concept of optimality with the concept of directionality. Directionality in edge detection is not a new concept. We would specifically like to mention the Kirsch and Robinson compass masks discussed in [4] and [5], which were influential for our formulation of the edge filtering problem.

Manuscript received February 15, 1996; revised April 15, 1997. The associate editor coordinating the review of this paper and approving it for publication was Dr. Maria Petrou.

The author is with the Department of Digital Systems, Monash University, Clayton 3168, Australia (e-mail: app@rdt.monash.edu.au).

Publisher Item Identifier S 1057-7149(98)02606-2.

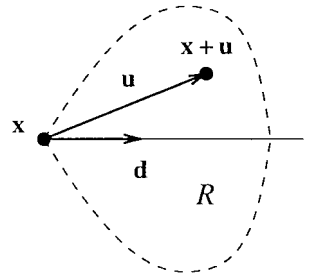

Fig. 1. Directional neighborhood of a pixel $\boldsymbol{x}$.

Formal considerations will be demonstrated using the so-called "posterior eye capsule images" discussed in [1] and [2]. Interpretation of these images facilitated the crystallization of the idea of directional filtering. Due to the nature of the underlying images, in which edges seem to be best modeled by the ramp transition in intensity, we based our directional filters on the 1-D Petrou–Kittler [16] edge filter, as the one that directly addresses the problem of detection of the ramp edges. Modification of our results for other types of edge detectors seems to be straightforward. As a projection function, we use a Gaussian window in a way similar to that presented in [12]. We show that, eventually, a 2-D n-directional edge filter can be represented by a pair of matrix filters, or equivalently by one complex-number filter, regardless of the number of filtering directions.

We start with the formalization of the concept of directional filtering and link it to the well-known Robert operator presented as a 2-D four-directional basic edge filter. In the next section we briefly review the Petrou–Kittler 1-D detector optimized for ramp edges, which is utilized in the subsequent sections, and discuss the 2-D extension using a projection function appropriately modified for directional filtering. Finally we present details of tridirectional 2-D filters and experimental results of their application for edge detection in the posterior eye capsule images. Relevant calculations were conducted using the MATLAB package [17].

II. Directional Filtering—Conjugate Images

Consider a neighborhood R of a pixel $\boldsymbol{x}$ expanded in the direction $\boldsymbol{d}$ as shown in Fig. 1. A general nonlinear filtering operation over the region R may now be defined by

$$f(\boldsymbol{x}) \longrightarrow g(\boldsymbol{x}; R) = \int_R h(f(\boldsymbol{x}+\boldsymbol{u}), \boldsymbol{u})\, d\boldsymbol{u} \tag{1}$$

where $f(\boldsymbol{x})$ and $g(\boldsymbol{x}; R)$ are the original and filtered images, respectively, described as functions of a vector variable, $\boldsymbol{x} = (x_1, x_2)$. Typically, such a region of interest is rotated in the directions $(\boldsymbol{d}_1, \cdots, \boldsymbol{d}_n)$ to cover the whole 2π angle. Applying the filtering operation (1) over the region R_{α_k}, we obtain a so-called *conjugate image*, $g_k(\boldsymbol{x})$. The edge strength may now be calculated by perform-

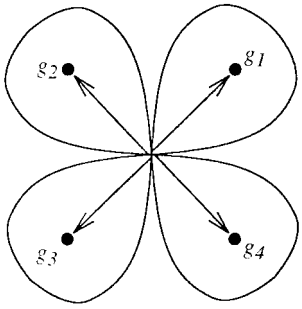

Fig. 2. Simplest four-directional filtering.

ing a vector addition of conjugate images. Using the complex-number notation, we have

$$e(\boldsymbol{x}) = \sum_{k=1}^{n} g_k(\boldsymbol{x}) e^{j\alpha_k} \tag{2}$$

where $e(\boldsymbol{x})$ is a complex-number-valued edge strength and its magnitude specifies a "standard" scalar edge strength.

If we use linear filters, then a conjugate image in the kth direction is calculated as a convolution of the original image, $f(\boldsymbol{x})$, with a kth directional filter, $h_k(\boldsymbol{x})$, as follows:

$$g_k(\boldsymbol{x}) = f(\boldsymbol{x}) \circ h_k(\boldsymbol{x}) \tag{3}$$

where '$\circ$' denotes the convolution operation. Now, the complex edge strength can be obtained as a convolution of the original image, $f(\boldsymbol{x})$, with the complex edge filter $h(\boldsymbol{x})$, as follows:

$$e(\boldsymbol{x}) = f(\boldsymbol{x}) \circ h(\boldsymbol{x}), \quad \text{where } h(\boldsymbol{x}) = \sum_{k=1}^{n} h_k(\boldsymbol{x}) e^{j\alpha_k} \tag{4}$$

where $h(\boldsymbol{x})$ is a sum of appropriately rotated filter components. This equation forms the basis of our further considerations.

As an introductory example, let us consider the conceptually simplest directional filtering as presented in Fig. 2.

In this case, there are four directions, $(2k-1)(\pi/4), k = 1, \cdots, 4$, thus four filtering regions, each of which containing precisely a single pixel of the image. The edge pixel is selected to lie between the image pixels. If the image is $f(\boldsymbol{x})$, where $\boldsymbol{x} = (x_1, x_2)$, then four conjugate images are specified as

$$g_1(\boldsymbol{x}) = f(\boldsymbol{x} + [0,1]), \quad g_2(\boldsymbol{x}) = f(\boldsymbol{x})$$
$$g_3(\boldsymbol{x}) = f(\boldsymbol{x} + [1,0]), \quad g_4(\boldsymbol{x}) = f(\boldsymbol{x} + [1,1])$$

where it is assumed that images are presented in the "matrix" coordinates, x_1 and x_2 being the row and column coordinates, respectively. In addition the origin of the edge strength image is shifted diagonally up and left by the 0.5 unit. The filtering operations which induce the "conjugate images," g_k are, in this case, simple identity operations with appropriate shifts as shown in the equations above. The complex edge map can be obtained using (2) as

$$e(\boldsymbol{x}) = \sum_{k=1}^{n} g_k(\boldsymbol{x}) e^{j(2k-1)\pi/4}.$$

At this stage, it seems to be convenient to use a matrix notation, in which a capital letter, say F, will represent a matrix of samples of an equivalent function, $f(\boldsymbol{x})$. Using this notation, a matrix representing the complex edge map, E, can now be determined using a discrete convolution as

$$E = F \circ H. \tag{5}$$

TABLE I
PARAMETERS OF THE PETROU–KITTLER 1-D FILTER

l	b	r_1	r_2	α_1	α_2	a
2	0.2628	1.3042	0.0946	−0.0166	1.1191	1.42
3	0.9437	2.0338	0.1200	0.2370	1.2897	0.9
4	0.9452	2.1682	0.1062	0.4149	1.1942	0.7
5	0.9881	2.5047	0.1081	0.6282	1.2070	0.56
6	0.8050	2.5226	0.1049	0.7510	1.1889	0.47
7	0.6421	2.4753	0.0979	0.8230	1.1367	0.41

The complex "four-directional" filter, H, can be directly determined using (4) by adding four uni-directional components, namely

$$H = \begin{bmatrix} 0 & 1 \\ 0 & 0 \end{bmatrix} \cdot e^{j\pi/4} + \begin{bmatrix} 1 & 0 \\ 0 & 0 \end{bmatrix} \cdot e^{j3\pi/4} + \begin{bmatrix} 0 & 0 \\ 1 & 0 \end{bmatrix} \cdot e^{j5\pi/4} + \begin{bmatrix} 0 & 0 \\ 0 & 1 \end{bmatrix} \cdot e^{j7\pi/4}. \tag{6}$$

Therefore

$$H = \begin{bmatrix} j & 1 \\ -1 & -j \end{bmatrix} \cdot e^{j\pi/4}. \tag{7}$$

The four-directional filter of (7) can be thought of as a complex extension of the Roberts edge operators [4]. Note that the filter of (7) is not symmetrical and care must be taken using the convolution operation versus a "mask" operation. Finally, it is possible to rewrite (6) and (7) in a direct form as

$$E = e^{j(\pi/4)}((G_3 - G_1) + j(G_4 - G_2)). \tag{8}$$

From this equation, the result is predictable and intuitively obvious, and can be restated that in order to calculate the edge strength, we subtract the pixel values lying in the opposing directions of the reference point. From (8) it can be noted that if any four neighboring pixels are identical the corresponding edge pixel is zero.

At the conclusion of this section, one comment on "conjugate images," g_1, g_2, g_3, g_4, can be made. In the application to edge extracting the need for creating four images, which are primarily identical to the original image, may not be obvious. However, two points can be made to emphasize the method. First, it seems that by creating conjugate images, we parallelize, at least conceptually, calculations from the pixel-by-pixel fashion to operations with whole images. Second, and most important, the conjugate images can be conveniently used to form multidimensional (four-dimensional, in this case) histograms of intensity, that is co-occurrence arrays used in image segmentation.

III. OPTIMAL DIRECTIONAL FILTERS

Dealing with imperfect edges, characterized either by a gradual transition in intensity, or blurred by noise, the calculation of the intensity gradient is combined with appropriate lowpass filtering. From a collection of available optimal filters listed in the introduction, we have based our specific calculations on a Petrou–Kittler 1-D edge filter [16], because it specifically targets the ramp edges which seem to be prevalent in our images.

In the Petrou–Kittler model the 1-D edge filter, from which we will use only the "positive" half, is optimized for the unified ramp edges and is specified by the following expression:

$$s(r) = 1 + be^{-r} - r_1 e^{ar}\cos(ar + \alpha_1) + r_2 e^{-ar}\cos(ar + \alpha_2) \tag{9}$$

where $0 \le r \le l, l$ is the span of the filter, that is, $s(0) = 0$ and $s(l) = 0$. For $l = 2, \cdots, 7$, the filter parameters are given in Table I.

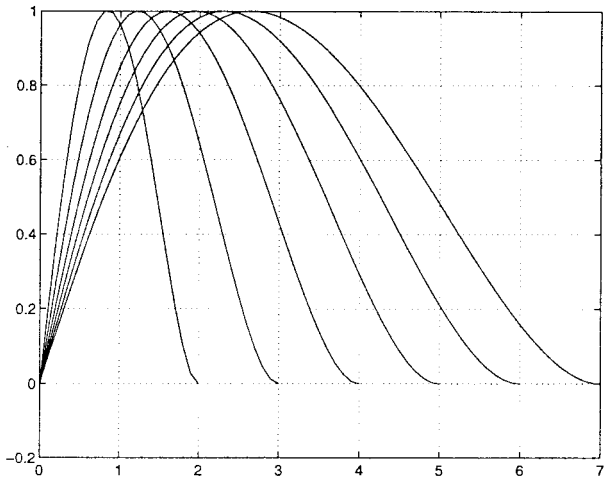

Fig. 3. One-dimensional Petrou–Kittler edge half-filters for various spans, l, as specified by (9).

The 1-D edge half-filters as specified by (9), are plotted for various span parameters and shown in Fig. 3.

Extension of a 1-D filter to two dimensions is typically performed by applying the edge filter in the direction perpendicular to the edge, and a projection function along the edges. A projection function should be a windowed lowpass filter, and two choices are most appealing, namely, the use of either the integral of the optimal edge filter as in [13], or the Gaussian function as in [12]. For simplicity, we opted for the latter only expressed in the polar coordinates which seem to be more natural for directional filtering. Therefore, the 2-D edge half-filter $h(\boldsymbol{u})$, which will be a building block of the 2-D directional edge filters, is composed from the Petrou–Kittler edge detector applied in the radial direction, and the Gaussian function applied in the angular direction. Using the complex-number notation, we have

$$h(\boldsymbol{u}) = \eta \cdot s(r) \cdot p(\theta), \quad \boldsymbol{u} = re^{j\theta} \tag{10}$$

where η is the normalization constant, and the pixel vector $\boldsymbol{u}$ is specified by its radial and angular components, r and θ. The radial component of a 2-D filter, $s(r)$, is specified in (9), whereas the angular component is

$$p(\theta) = e^{-c_\theta \theta^2}. \tag{11}$$

The angular spread of the of the filter is controlled by c_θ. For n-dimensional filtering, c_θ is chosen so that the factor $p(\theta) = \delta$ if the angular deviation from the central direction of the filter is $\theta = \pm(\pi/n)$. Therefore

$$c_\theta = \left(\frac{n}{\pi}\right)^2 \ln \frac{1}{\delta} \tag{12}$$

Such a choice of the Gaussian window with the angular spread constant, c_θ, gives rise to intended overlapping of directional filters. The degree of overlapping is controlled by δ. The value of the angular component, $p(\theta)$, at the centre of the adjacent region is $p(2\pi/n) = e^{4 \ln \delta} = \delta^4$. For a typical value, $\delta = 0.5$, we have $p(2\pi/n) = 1/16$.

IV. Tridirectional Filters

At first glance, it seems that in order to estimate two components of the intensity gradient, that is, to determine the edge map, four filtering directions, e.g., $(0, 90, 180, 270^\circ)$ might be required. However, at the close examination it appears that three directions, e.g., $(0, 120, 240^\circ)$, constitute the sufficient basis for the gradient calculation. Conceptually, in order to estimate gradient, we usually use an antisymmetric mask in two orthogonal directions. Our method of tridirectional filtering involves a vector sum of three halves of such a mask in order to estimate the edge strength vector.

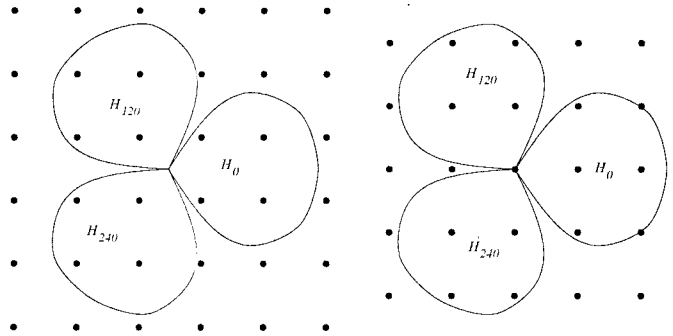

Fig. 4. Two variants of tridirectional filtering for $l = 2$. The left variant implies a 4×4 filter, whereas the right one involves a 5×5 filter.

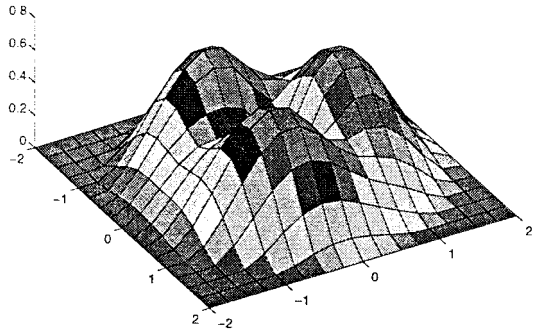

Fig. 5. Tridirectional filter for $l = 2$ and $\delta = 0.5$.

As an example of tridirectional edge filtering consider the pixel arrangements as shown in Fig. 4.

The three components of the tridirectional filter can be determined from (10) for a given radial span, l, and the angular spread controlled by the overlapping factor, δ. Let the three sampled filter components be H_0, H_{120}, H_{240}, respectively. Then the complex edge filter can be calculated as

$$H = H_0 + H_{120} \cdot e^{j2\pi/3} + H_{240} \cdot e^{-j2\pi/3}. \tag{13}$$

The complex matrix mask, H, includes all three filtering directions and is of a size, either $(2l+1) \times (2l+1)$ if the center of the mask is located at the reference pixel (the right part of Fig. 4), or $2l \times 2l$ if the interpixel position of the mask is selected (the left part of Fig. 4).

As a specific example consider a tridirectional filter calculated using (10) and (13) for $l = 2$ and $\delta = 0.5$. Its magnitude is plotted in Fig. 5.

If we position such a filter as in the left part of Fig. 4, the resulting 2-D tridirectional edge filter can be described by the 4×4 complex matrix of the form

$$H = \begin{bmatrix} 0 & -52 & 7 & 0 \\ -65 & -179 & 178 & 110 \\ -65 & -179 & 178 & 110 \\ 0 & -52 & 7 & 0 \end{bmatrix} + j \begin{bmatrix} 0 & 104 & 70 & 0 \\ 46 & 255 & 101 & 12 \\ -46 & -255 & -101 & -12 \\ 0 & -104 & -70 & 0 \end{bmatrix}. \tag{14}$$

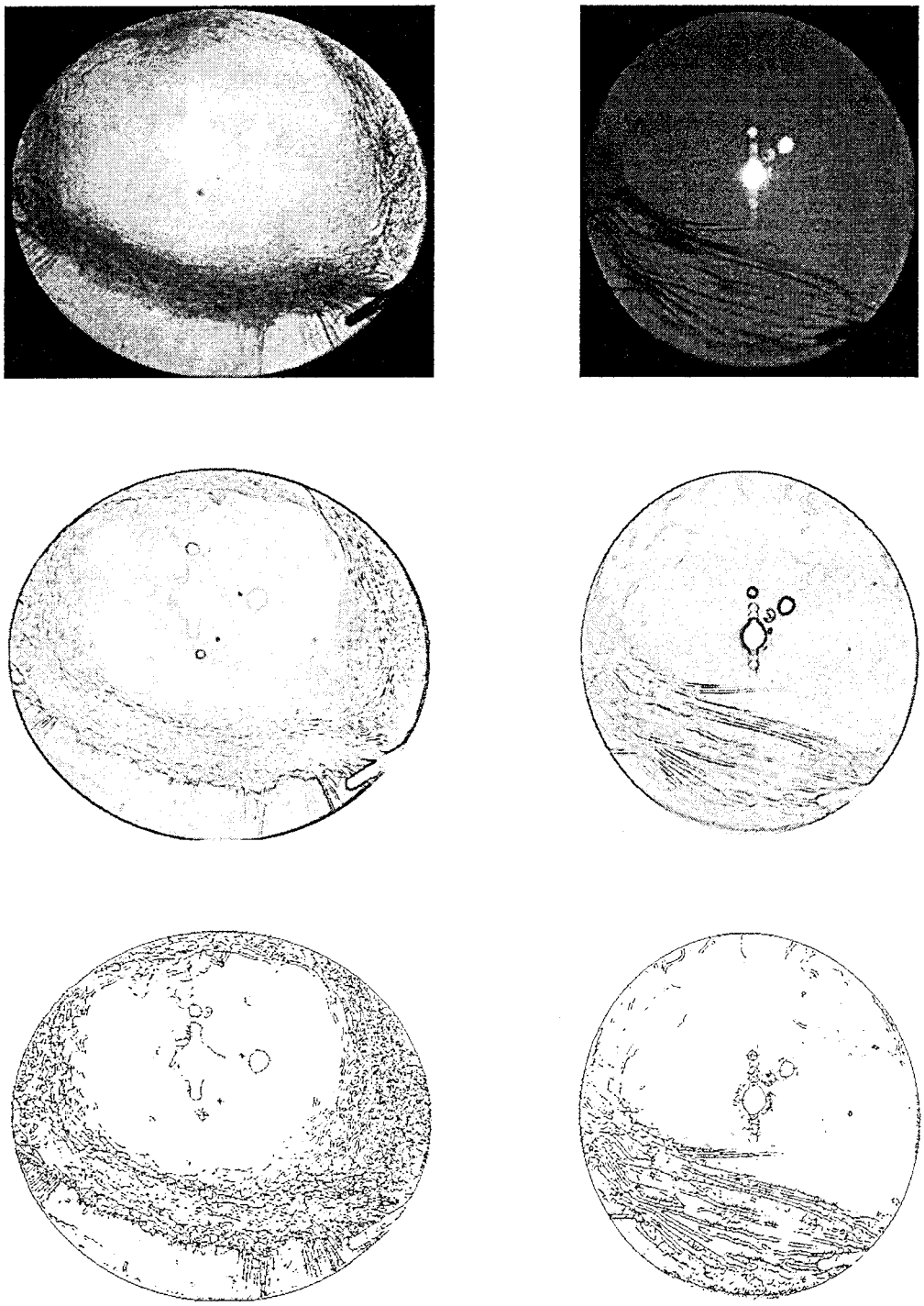

Fig. 6. Top row: test images. Middle row: magnitude of the edge strength obtained using a tridirectional filter of (14) with span $l = 2$. Bottom row: edge maps after thinning and thresholding operations.

The filter of (14) has been truncated to the 8-b representation and expressed in integer numbers. From (14), it is possible to note the three tear-drop regions characterized by the groups of four top-left, bottom-left and middle-right matrix entries.

The above filter $(n = 3, l = 2, \delta = 0.5)$ has been tested with the posterior eye capsule images and some results are presented in Fig. 6.

The first row of Fig. 6 depicts two posterior eye capsule images. These images describe the degree of opacification of the membrane behind an artificial lens inserted during the cataract operation. The membrane may become opaque, which results in blurred vision. The second row illustrates the edge strength maps generated using convolution of images with the tridirectional filter of (14). In the third row, the above maps are presented after operations of thinning the edges and their thresholding have been performed. The thinning is achieved by applying a simple operation of edge erosion in which all pixels that are, together with their neighbors, located on a slope of the edge map, are set to zero. This leaves only one-pixel wide edges, which are subsequently unified by thresholding. In general, the edge map does not describe very well the complex structure of the posterior capsule images, which typically lack any prominent features.

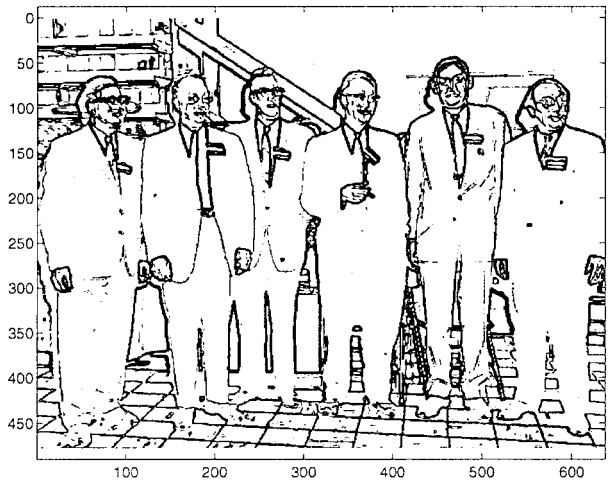

Fig. 7. Magnitude of the edge map of the Gatlin image obtained using a tridirectional filter of (14).

In reality, the edge operators are used to perform segmentation of such images [2], rather than to obtain the structure of edges.

Finally, the tridirectional edge filter of (14) has been applied to an image called "Gatlin" from MATLAB, representing a photo of a group of people. The resulting edge map for this image, thresholded at the level of 10% of the maximum value, is presented in Fig. 7. In this case, edges are naturally better defined and are prominent enough without additional thinning operation.

V. Conclusion

We have discussed how, starting from a selected model of a 1-D optimal edge detector, to build a 2-D edge filter that collects information from n directions around a central pixel. The 2-D filter is specified by three parameters, the number of filtering directions, n, the radial span, l, and the angular overlap factor, δ. Computationally, such a 2-D n-directional optimal filter can be represented by a $2l \times 2l$ complex matrix, which is equivalent to two real filters, regardless of the number of filtering directions.

As an underlying 1-D edge detector, we selected a Petrou–Kittler model [16] that directly addresses the ramp edges characteristic to the class of medical images of interest.

Specific calculations were conducted for a tridirectional 2-D edge filter that offers the smallest possible number of filtering directions. The tridirectional filtering is specifically attractive in the context of segmentation of images because it delivers the smallest possible dimensionality (three) of a co-occurrence array that is able to describe completely the distribution of information around a given pixel. This aspect is discussed in greater detail in [18]. See also [2].

Acknowledgment

The author expresses gratitude to D. J. Spalton from the Department of Ophthalmology, St. Thomas' Hospital, London, U.K., for the provision of the eye images.

References

[1] A. P. Papliński and J. F. Boyce, "Computational aspects of segmentation of a class of medical images using the concept of conjugate images," Tech. Rep. 95–6, Dept. Roboti. Digital Technol., Monash University, Clayton, Australia, Apr. 1995.

[2] ——, "Segmentation of opacification of posterior capsule images," in *Proc. 3rd Conf. Digital Image Computing: Techniques and Applications, DICTA95*, Brisbane, Australia, Dec. 1995, pp. 503–508.

[3] R. C. Gonzalez and R. E. Woods, *Digital Image Processing*. Reading, MA: Addison-Wesley, 1992.

[4] R. M. Haralick and L. S. Shapiro, *Computer Vision*, vol. 1. Reading, MA: Addison-Wesley, 1992.

[5] A. K. Jain, *Fundamentals of Digital Image Processing*. Englewood Cliffs, NJ: Prentice-Hall, 1989.

[6] D. Marr and E. Hildreth, "Theory of edge detection," in *Proc. R. Soc. Lond. B*, vol. 207, pp. 187–217, 1980.

[7] J. Canny, "A computational approach to edge detection," *IEEE Trans. Pattern Anal. Machine Intell.*, vol. PAMI-8, pp. 679–698, Nov. 1986.

[8] F. van der Heijden, "Edge and line feature extraction based on covariance models," *IEEE Trans. Pattern Anal. Machine Intell.*, vol. 17, pp. 16–33, Jan. 1995.

[9] R. Deriche, "Using Canny's criteria to derive a recursively implemented optimal edge detector," *Int. J. Comput. Vis.*, vol. 1, pp. 167–187, 1987.

[10] J. Shen and S. Castan, "An optimal linear operator for edge detection," *CVGIP: Graph. Models Image Processing*, vol. 54, pp. 112–133, Mar. 1992.

[11] ——, "Toward the unification of band-limited derivative operators for edge detection," *Signal Process.*, vol. 31, pp. 103–119, 1993.

[12] K. R. Rao and J. Ben-Arie, "Optimal edge detection using expansion matching and restoration," *IEEE Trans. Pattern Anal. Machine Intell.*, vol. 16, pp. 1169–1182, Dec. 1994.

[13] S. Sarkar and K. L. Boyer, "On optimal infinite impulse response edge detection filters," *IEEE Trans. Pattern Anal. Machine Intell.*, vol. 13, pp. 1154–1171, Nov. 1991.

[14] R. Boie and I. Cox, "Two dimensional optimum edge recognition using matched and Wiener filters for machine vision," in *Proc. Int. Conf. Computer Vision*, London, U.K., 1997, pp. 450–456.

[15] L. A. Spacek, "Edge detection and motion detection," *Image Vis. Comput.*, vol. 4, pp. 43–56, Feb. 1986.

[16] M. Petrou and J. Kittler, "Optimal edge detectors for ramp edges," *IEEE Trans. Pattern Anal. Machine Intell.*, vol. 13, pp. 483–491, May 1991.

[17] *MATLAB Reference Guide*. Natick, MA: MathWorks, 1994.

[18] A. P. Papliński, "N-directional filtering in image segmentation based on co-occurrence arrays," Tech. Rep. 96–9, Dept. Digital Syst., Monash Univ., Clayton, Australia, Apr. 1996.